A Software Tool to automatically evaluate and quantify Diffusion Weighted Images

D. Simon[1], J. Klein[2], J. Rexilius[2], T. Re[3], A. Lemke[4], F. Laun[5], B. Stieltjes[3]

[1] German Cancer Research Center, Software Development for Integrated Diagnostics and Therapy, Heidelberg, Germany
[2] Fraunhofer MEVIS, Bremen, Germany
[3] German Cancer Research Center, Department of Radiology, Heidelberg, Germany
[4] Chair in Computer Assisted Clinical Medicine, University of Heidelberg, Faculty of Medicine, Mannheim, Germany
[5] German Cancer Research Center, Department of Medical Physics in Radiology, Heidelberg, Germany

Abstract— **Diffusion weighted imaging (DWI) derived apparent diffusion coefficient (ADC) is currently used in identifying and post-therapy followup of several types of tumours. In brain tumours in particular ADC values are known to correlate inversely to tumour cellularity and high and low malignant areas can be distinguished based on ADC values.**

The average ADC value increases after successful chemotherapy, radiotherapy or a combination of both and is used as a surrogate marker for treatment response.

More recently DWI derived ADC has been used to differentiate pancreatic cancer from healthy pancreatic tissue although with some limitations. A second DWI derived parameter, the perfusion fraction *f* has also shown promise in classifying pancreatic lesions. This parameter is estimated using special multiple b-value prototypes and the IVIM model.

The main purpose of our project was to develop a software platform to assist radiologists in studying cancerous lesions by quantifying and mapping these two DWI derived parameters: ADC and perfusion fraction *f*. The platform we developed automatically calculates and maps the ADC and IVIM-model perfusion fraction *f* values from raw diffusion data.

Furthermore, the software enables the automated delineation and ADC quantification of tissue sections in a fast, objective, user independent manner and has so far been applied to successfully delineating brain tumours. The perfusion fraction *f* mapping capabilities have so far been successfully applied to delineate pancreatic cancer lesions from healthy tissue. Further studies are in preparation to apply this software tool to study both ADC and perfusion fraction *f* in other types of cancerous lesions.

Keywords— **Diffusion Weighted Imaging, EM-Clustering, Gaussian Mixture Model, IVIM Model, Gliomas, Pancreatic Cancer**

I. Introduction

Diffusion weighted magnetic resonance imaging [1,2] (DWI) is a method of micro anatomical imaging and was introduced into clinical practice in 1990. In this method the Brownian molecular motion of water is measured. Diffusion can be classified into two principal types: isotropic, in which diffusion occurs in all directions equally (as occurs in free diffusing water), and anisotropic in which diffusion occurs unequally along different directions (as occurs in fiber rich biological tissues in which the diffusion is most prominent parallel to the fibers). Diffusion Weighted Imaging (DWI) is the qualitative representation of the diffusion information in a tissue under examination [1]. In DWI a number of quantification steps can be distinguished but two basic measurements can be delineated. The first measurement entails scalar values which are recorded as a so called apparent diffusion coefficient ADC map. In this map, the diffusion coefficients are averaged for each voxel. The second method determines a diffusion tensor from at least six values from an orthonormal basis of eigenvectors. In this article, only the second case is being considered as the data is restricted to scalar values shown that "diffusion weighted measurements" actually reflect microscopic molecular motion due to both diffusion and to micro perfusion [4], [5].

In his publication of 2008 [6], Le Bihan recalls the important meaning of the IVIM Model in the focus of modeling the movement of blood in the microvasculature as a pseudodiffusion process on a macroscopic scale. It can be clearly demonstrated that the pseudodiffusion process is much higher than the usually considered molecular diffusion. Thus, the microperfusion contributes to the measured apparent diffusion only when low b-values are used and is therefore a marker for motion sensitization physical properties of the applied gradient scheme. Lemke et al. have shown that the IVIM Model perfusion fraction *f* parameter can be used to successfully delineate between pancreatic cancer and healthy tissue, thanks to the typically hypoperfused nature of pancreatic tumours [7]. He also demonstrated, using a vascular suppression technique, that this perfusion parameter *f* is directly correlated to the vascular component in pancreatic tissue. Thus, we can assume that areas of where the perfusion fraction *f* is estimated to be very low correspond to areas of hypoperfusion which are likely areas of adenocarcinoma when occuring within obvious pancreatic lesions. Additionally, due to differences in the level of damage to tissue microcirculation caused by pancreatic cancer when compared to pancreatitis, the perfusion fraction *f* parameter can likely be used in the differentiation of lesions caused by these two different pathologies.

Chenevert and colleagues demonstrated that the ADC is inversely correlated to cellularity in brain tumours [9].

It has been shown that the ADC increases after successful chemotherapy, radiotherapy or a combination of both. There, the mean ADC can be seen as a surrogate treatment marker. A high proliferating tumour results in a low ADC mean value whereas a low proliferation tumour shows a high ADC mean value.

Moreover, the ADC mean can also be used to separate high and low malignant areas in gliomas [10].

Delineation between high and low malignant areas is important for resections, biopsies and radiation therapy [11]. In current practice, such delineation is usually performed by means of manual region of interest (ROI) selection and is therefore highly operator dependent. Furthermore, ADC quantification within a ROI quantification is impeded by poor data resolution and a low contrast between high and low malignant areas. Hence, an automatic and robust ADC based tissue segmentation is of strong interest.

In a work we presented at the Proceedings of SPIE Medical Imaging (2009),[12] we demonstrated that the level of tumour heterogeneity can be determined in an objective manner with minimal physician input. In this work, the Gaussian distributions in the different tumour areas were identified and through the application of an Expectation Maximization algorithm with Gaussian mixture model an objective delineation of these regions was achieved.

At our center in Heidelberg, the German Cancer Research Center, there is a strong need to foster a unified software platform capable of meeting the needs of several radiodiagnostics and radiotherapy research groups. Important is the integration of a common data handling software capable of seamlessly accessing and manipulating data from a common research dedicated PACS. Also essential is a common interface to ensure consistency and convenience for the users and minimal maintenance effort on the part of the IT department. Furthermore, an automatic, advanced preprocessing of the raw data to easily access pre-evaluated images is mandatory.

Thus, necessary preprocessing, data analysis steps and software tools from research projects are being integrated into one general software platform called “DIROlab” (Diagnostic Imaging in Radio-Oncology Lab) which is based upon the software development platform “MeVisLab” [13].

II. Advanced Preprocessing

The developed software allows for automatic preprocessing. That means that the diffusion raw data is automatically processed to determine the ADC map. For each of the integrated scanner pulse sequence protocols listed in Table 1 incorporates a calculation of the ADC. Unfortunately, the calculated value of ADC for a given voxel was not able to obtain directly from the scanner. The software therefore incorporates a new consistent calculation of ADC directly from the scanner's raw data.

Table 1 MR-Sequences

Sequence Type	Diffusion Sequence
ECHO PLANAR IMAGING	DIFFMODE_ORTHOGONAL DIFFMODE_SLICE DIFFMODE_READ DIFFMODE_PHASE DIFFMODE_THREE_SCAN_TRACE DIFFMODE_TENSOR
HASTE	DIFFMODE_DIAGONAL DIFFMODE_ORTHOGONAL DIFFMODE_SLICE DIFFMODE_READ DIFFMODE_PHASE

For automatic determination of the ADC map, we use several equations based on the input data type.

For DIFFMODE_ORTHOGONAL we are using the following equation:

$$< ADC >= \frac{ADC_x + ADC_y + ADC_z}{3} \quad (1)$$

Where $$ADC = \frac{-1}{b} \cdot \ln\left(\frac{S}{S_0}\right) \Leftrightarrow \quad (2)$$

$$< ADC >= \frac{1}{3} \cdot \frac{-1}{b} \cdot \left(\ln\left(\frac{S_x}{S_0}\right) + \ln\left(\frac{S_y}{S_0}\right) + \ln\left(\frac{S_z}{S_0}\right)\right). \quad (3)$$

The mean ADC in the orthogonal directions *read*, *phase*, *slice* is being calculated and anisotropic traits are being prevented.

For DIFFMODE_SLICE and DIFFMODE_DIAGONAL (gradient applied in direction $\begin{pmatrix}1\\1\\1\end{pmatrix}$) equation 2 is being used and thus provides an ADC calculation in only one direction. Unfortunately, the result is impeded by anisotropic traits.

The trace image can be derived from equation 2. The trace calculation itself is shown in equation array 4.

$$< ADC >= \frac{-1}{3} \cdot \frac{\ln\left(\frac{S_x}{S_0}\right) + \ln\left(\frac{S_y}{S_0}\right) + \ln\left(\frac{S_z}{S_0}\right)}{b} \Leftrightarrow \quad (4)$$

$$< ADC >= \frac{-1}{3} \cdot \frac{\ln(S_x \cdot S_y \cdot S_z) - 3 \cdot \ln(S_0)}{b} \Leftrightarrow$$

$$< ADC >= -\frac{\ln(S_x \cdot S_y \cdot S_z)^{\frac{1}{3}} - \ln(S_0)}{b}$$

where $S = (S_x \cdot S_y \cdot S_z)^{\frac{1}{3}}$ denotes the trace, hence, $< ADC >= -\frac{\ln\left(\frac{S}{S_0}\right)}{b}$. For DIFFMODE_TENSOR and an array of *trace weighted images* we determine the ADC by linear least squares calculation.

Thus, for tensor calculation, we are using the following equation:

$$\begin{aligned} &\ln(S) = \ln(S_0) - D \cdot b \Leftrightarrow \\ &\hat{\theta} = \begin{pmatrix} \hat{\alpha} \\ \hat{\beta} \end{pmatrix} = (X^T \cdot X)^{-1} X^T \cdot (\ln(S) - \ln(S_0)) \Leftrightarrow \\ &\hat{\theta} = \begin{pmatrix} \hat{\alpha} \\ \hat{\beta} \end{pmatrix} = X^+ \cdot (\ln(S) - \ln(S_0)). \end{aligned} \tag{5}$$

The matrix X comprises the b-value and gradient directions.

For several *trace weighted images* the calculation is denoted as follows:

$$\begin{aligned} &\vec{y} = \begin{pmatrix} \ln(s_1) \\ \ln(s_2) \\ \vdots \\ \ln(s_n) \end{pmatrix} = \begin{pmatrix} 1 & b_1 \\ 1 & b_2 \\ \vdots & \vdots \\ 1 & b_n \end{pmatrix} \cdot \begin{pmatrix} \hat{\alpha} \\ \hat{\beta} \end{pmatrix} + \begin{pmatrix} e_1 \\ e_2 \\ \vdots \\ e_n \end{pmatrix} \Leftrightarrow \\ &\hat{\theta} = ((X^T \cdot X)^{-1}) \cdot X^T \cdot \vec{y} \Leftrightarrow \\ &\hat{\theta} = X^+ \cdot \vec{y}. \end{aligned} \tag{6}$$

III. Objective tumour heterogeneity determination

A. Initialization and preprocessing steps

The application allows for an objective tumour heterogeneity determination in gliomas.

In [12] and [14] we proved and showed that an Expectation Maximization algorithm with a Gaussian mixture model can be applied to objectively delineate low malignant from high malignant tumour. Moreover, in [12] is described that the seed point, which is the initialization of the algorithm, does not interfere with the clustering result.

The procedure of the clustering is shown in [14]. Firstly, the data is processed in to determine the ADC map. We used equation (5) to perform the quantification. In theprocess, we used T1 weighted and T2 FLAIR images as a ground truth. To match the ADC and the T1 weighted and the T2 FLAIR image, we used a linear rigid registration algorithm and the normalized mutual information metric.

Next, the GTV (Gross Tumour Volume) is determined upon the T1 weighted and T2 FLAIR weighted image, respectively and the overlaying ADC map. Then, the two malignant areas are clustered with help of an Expectation Maximization algorithm and a Gaussian mixture model.

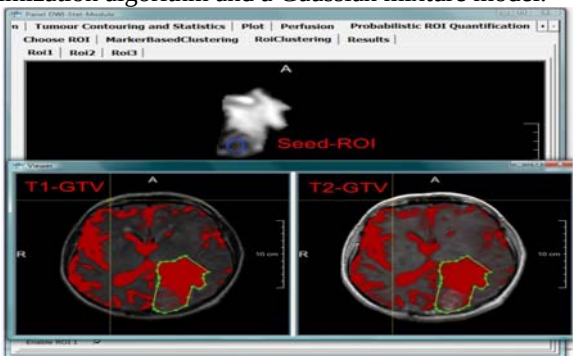

Fig. 1: T1 and T2 FLAIR image with overlaying ADC map in red, seed ROI definition and defined GTV by the physician (see [14])

B. The EM algorithm with Gaussian mixture model

The EM algorithm with Gaussian mixture model incorporates two steps, namely the Expectation and the Maximization step, respectively.

In the Expectation step the cluster probabilities are being determined, i.e. γ_k is being calculated.

$$\begin{aligned} &\gamma_k(x) \equiv p(k \mid x) \\ &= \frac{p(k)p(x \mid k)}{\sum_{k=1}^{K} p(k)p(x \mid k)} \\ &= \frac{p(k)p(x \mid k)}{\sum_{k=1}^{K} \pi_k \mathrm{N}(x \mid \mu_k, \Sigma_k)} \end{aligned} \tag{7}$$

Here, the Bayes Theorem is being used to calculate the cluster probabilities.

$\sum_{k=1}^{K} \pi_k \mathrm{N}(x \mid \mu_k, \Sigma_k)$ comprises the total probability and represents the whole Gaussian mixture model.

The Maximization step uses the posterior probability to recalculate the model parameters. (π_k, Σ_k, μ_k) Then, we do have the following Log likelihood equation to maximize:

$$\ln(p(x \mid \mu, \Sigma, \pi) = \sum_{n=1}^{N} \ln\left\{\sum_{k=1}^{K} \pi_k \mathrm{N}(x \mid \mu_k, \Sigma_k)\right\} \tag{8}$$

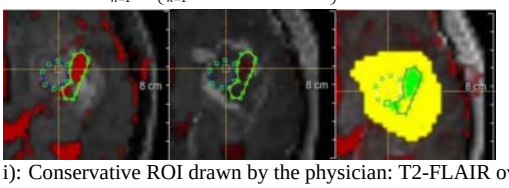

Fig. 2: i): Conservative ROI drawn by the physician: T2-FLAIR overlaid with ADC map in red, (ii): Conservative ROI drawn by the physician: T1 overlaid with ADC map in red. The blue circle indicates the conservative high malignant area, the yellow circle indicating the low malignant

area, (iii): Clustered area: yellow indicates the posterior probability (γ_k) for the high malignant area (see [12])

C. Refining the clustering result

We encountered some problems concerning the clustering result. First, overlaps were found in the range of intensities representing tumour and normal tissue. Second, overlaps between the intensities of low malignant tissue and cerebrospinal fluid were identified.

For the second issue we found a solution in [12] with the application of a binary T2 FLAIR mask. Thus, the cerebrospinal fluid is completely suppressed in the clustering results. The first issue still remains unsolved and in [12] we consider some options, such as using more sophisticated algorithms with pre knowledge.

IV. A TOOL MAINLY DESIGNED FOR THE DELINEATION OF PANCREATIC TUMOUR

A second important use of our software tool was in the diagnosis of pancreatic tumours based on the perfusion component of the diffusion weighted signal decay [I]. Pancreatic tomours are typically seen as hypoperfused areas in contrast CT and MRI studies. As there is a safety risk associated both with the ionizing radiation of CT and the use of contrast agent in both CT and MRI, a non-contrast agent MRI technique was desired. Diffusion weighted imaging (DWI) is a MRI technique which does not require contrast agent and is influenced by the amount of perfusion of the studied tissue [5]. We therefore decided to quantify the perfusion component of the DW-data to use in the delineation of hypoperfused pancreatic lesions. Several different techniques were used to extract the perfusion component from the DW-data. Specifically, we established the following methods to qualitatively and or quantitatively represent the perfusion component of the DW-data:

Determining the R-Squared value which denotes the linearity of the decaying signal, $\ln\left(\frac{S}{S_0}\right)$ against b, resulting in $R^2 = 1 - \frac{C_R}{C_y}$. Calculating the integral between the linear least squares calculation and the real signal decay denoted by $\ln\left(\frac{S}{S_0}\right)$ against b only considering b-values below 150 $\left[\frac{s}{mm^2}\right]$, following [15]. We used the Simpsons rule to perform an approximated calculation of the integral. Thus, the approximated integral is denoted as follows:

$$\int_0^{150} f(x)dx \approx \frac{150}{n}\left(\frac{f(150)-f(0)}{2} + \sum_{k=1}^{n-1} f\left(0 + k \cdot \frac{150}{n}\right)\right)$$ .f(x) is describing the signal decay.

Using the IVIM-Model [1] and determined the F parameter. Specifically, we used a Levenberg Marquardt algorithm and an analytically determined Jacobian descent, as a non linear least squares method, to fit the IVIM function denoted as follows:

$\frac{S}{S_0} = (1-f)\cdot e^{-bD} + fe^{-b(D+D^*)}$ where *f* represents the perfusion fraction or the volume fraction of the capillary vessels in a voxel and was the most prominent candidate for delineation [I]. D* denotes the pseudo diffusion constant which is connected to the velocity of the blood.

Each of these methods were used to generate perfusion maps of DW-data and are currently being evaluated for pancreatic cancer delineation.

V. CONCLUSIONS

An application capable of an automatic ADC determination and to efficiently delineate high malignant from low malignant tumour in gliomas and moreover to delineate pancreatic cancer from normal pancreatic tissue in an efficient way was presented. Thus, providing an application to conveniently preprocess and postprocess diffusion weighted images in a scalar way.

REFERENCES

1. Tofts P, “Quantitative MRI of the Brain, Measuring changes caused by disease”, Wiley (2003)
2. Mori S, „Introduction to Diffusion Tensor Imaging“, Elsevier (2007)
3. Matsuki M, Abdom Imaging, (2007), 32(4):481-483
4. Lee SS, J Magn Reson Imaging 2008; 28(4):928-936
5. Le Bihan D, Radiology, (1988), 168(2):497-505
6. Le Bihan D, Radiology, (2008), 249(3): 748-752
7. Lemke A, Proceedings 17th Scientific Meeting, ISMRM, Honolulu , 2009, p.666
   Lemke A, Proceedings 17th Scientific Meeting, ISMRM, Honolulu , 2009, p.1365
8. Chenevert, T. L., J Natl Cancer Inst., (2000), 92(24):2029– 2036
9. Brunberg, e. a., (1995) American Society of Neuroradiology, 16(2):261-71
10. Stadnik, e. a., AJNR (2001) 22(5):969-976
11. Simon D., e.a., Proceedings of SPIE Medical Imaging 2009, Vol. 7260, 72601X-1– 72601X-9, Orlando, USA, 2009, DOI:10.1117/12.812521
12. MeVisLab 2.0 Release Candidate, “Homepage at: http://www.mevislab.de. Accessed June, 2009.”
13. Simon D., e. a., “Towards User-Independent ADC Quantification in Gliomas”, ESMRMB (2008)
14. Siemens Medical, “Magnete Spins und Resonanzen, Eine Einführung in die Grundlagen der Magnetresonanztomographie“, Siemens AG (2003)